Angular and radial relaxation of a crystal lattice around a nonspherical impurity: The KI:NO_3 system under uniaxial stress

J. Bruining and J. van der Elsken
Laboratory for Physical Chemistry, University of Amsterdam, The Netherlands
(Received 24 December 1974)

In single crystals of KI containing NO_3^- impurities in concentrations of 10^{18} per cm^3 two gap modes can be observed as combination bands with an internal mode of the nitrate ion. An experimental method has been developed to measure the gap-mode frequencies as a function of uniaxial stress while the crystal is held at liquid-helium temperature. Simple group-theoretical considerations lead to frequency strain derivatives for the two gap modes as well as for the internal mode. An isotopic substitution model in which angular and radial relaxation of the lattice around the impurity is taken into account can be used to calculate the two gap-mode frequencies as a function of this relaxation. Comparison with the experimental frequencies gives an angular relaxation from 90° to 81°40′ and a radial relaxation from 3.53 to 3.67 Å. The model also predicts the derivatives of the frequencies with respect to the relaxation at these values of the relaxation. A fair agreement with the experimental results is obtained.

I. INTRODUCTION

The study of localized vibrations of impurities in host lattices is an important means of investigation of the interaction potential between the impurity and the host lattices.[1,2] Knowledge of these potentials is of importance also for a better understanding of the properties of pure crystals. In the case of monoatomic impurities in pure ionic crystals like alkali-halide crystals, theoretical models have been fairly successful in explaining experimental observations such as far-infrared or near-infrared absorption spectra. Polyatomic impurities, however, have presented more difficulties.[3,4]

Knowledge of the angular dependence of the intermolecular potential of polyatomic ions in ionic crystals is of great importance. Many properties of pure crystals with complex ions are largely determined by the rotational degrees of freedom and hence by the angular dependence of the intermolecular potential. Since the application of uniaxial stress controls the symmetry around the impurity, the study of stress-induced changes of the localized vibrations is the obvious way to obtain information about this angular dependence. For monatomic impurities such studies have revealed considerable noncentral-force components for partially covalent bound ions, such as Ag^+ and Cu^+ in alkali halides.[5] The investigation of the stress effects on the frequencies of impurity modes associated with complex ions in simple alkali-halide crystals is, therefore, promising looking. The system KI: NO_3^- is the best known one in this field. The system has two gap modes, at 73 and 88 cm^{-1}, which have been observed in direct absorption in the far infrared[6] as well as in combination with an internal vibration of the nitrate ion in the near infrared.[4] Calculations on the basis of an isotopic substitution model have predicted a gap mode of 72 cm^{-1} and it has been assumed that the two gap modes observed arise from a lifting of the triply degenerate gap mode into an A- and an E-type mode. So far, no efforts have been made to give a quantitative explanation. In this paper we shall show how information can be obtained from the two gap-mode frequencies, about the angular dependence of the intermolecular potential. We shall furthermore present the experimental results of the stress-vs-frequency-shift measurements in the near infrared on the KI: NO_3^- system. From the experimental point of view it is a great advantage that the gap modes can be observed as combination bands in the near infrared. The high resolution which can easily be obtained in this frequency region allows the observation of very small shifts and hence the pressures that have to be applied can be kept small. This avoids the broadening of the lines resulting from nonuniform compressional stress and the consequent obscuration of the effects. The disadvantage of an investigation in the near infrared is that the gap-mode frequencies have to be found by subtraction. Careful analysis of the different possibilities that consequently may arise lead us to the conclusion that there is a satisfactory agreement between theory and experiment with regard to the stress-induced shifts.

II. EXPERIMENTAL

A. Techniques

Nitrate-doped crystals of KI were grown by the Kyropoulos method by adding 0.1-wt% KNO_3, to the KI melt. The concentration of the nitrate ions in the resulting crystals is of the order of 10^{18} nitrate ions per cm^3. Samples of the proper size, 15× 5× 5 mm, and desired orientation were ob-

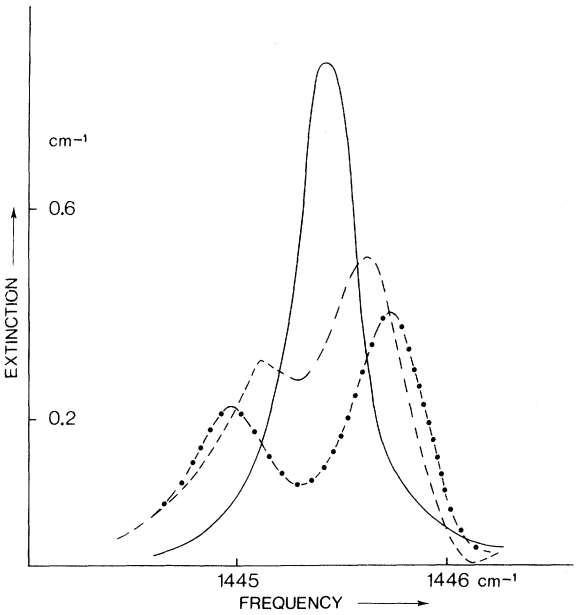

FIG. 1. Absorption band arising from the combination of the internal ν_3 vibration of the nitrate ion and the gap mode at 73 cm^{-1} under the influence of pressure in the [111] directions. $\vec{E} \parallel [110]$. Solid line, zero pressure; dashed line, 0.17 kbar; dash-dot line, 0.26 kbar.

tained by cleaving or cutting and by polishing the surfaces.

For the uniaxial-stress measurements a cryostat was constructed in which the pressure of helium gas is transferred to pressure on a crystal surface by means of bellows. The 0.02-mm-thick bellows were supported by a stainless-steel tube. The effective surface of the bellows was 1.9 cm^2. Bellows and crystal were immersed in a liquid-helium bath. The attained pressures were calibrated mechanically; the results turned out to be completely reproducible. Apparently the solidification of the helium in the bellows does not prevent a hydrostatic pressure transfer.

The optical measurements were carried out by using a Perkin Elmer E14 spectrophotometer equipped with a helium-cooled GeCu detector. The radiation was polarized by a golden-grid-wire polarizer. Depending on the remaining intensity with different polarization directions a resolution between 0.1 and 0.5 cm^{-1} could be obtained.

B. Spectra

The near-infrared spectrum of nitrate in KI between 1300 and 1500 cm^{-1} at liquid-helium temperatures has been published earlier.[7] Also the complicated structure of the spectrum has very satisfactorily been interpreted. The following sharp features are of importance for our purposes: the nitrate internal vibration band at 1372 cm^{-1} together with two combination bands at 1445 and 1460 cm^{-1}, and the internal vibration band of $^{15}NO_3^-$ at 1340 cm^{-1}. This last band appears in the spectrum due to the natural occurrence of ^{15}N. It is a low-intensity sharp line that monitors the shift of the internal vibration frequency especially if the 1372-cm^{-1} band of $^{14}NO_3^-$ is too intensive to be measured accurately. The combination bands at 1445 and 1460 arise from the 73- and 88-cm^{-1} gap modes as 1372+73 and 1372+88 cm^{-1}.

Using the methods outlined above we measured the frequency shift of the 1372- and 1340-cm^{-1} pure internal vibration bands and the combinations of the internal vibration with the two gap modes at 1445 and 1460 cm^{-1} as a function of stress. One example of the effect of uniaxial stress of a combination band is shown in Fig. 1. It is to be noted that in all cases the true bandwidth is smaller than the spectral bandwidth and hence the band shapes cannot be determined. The absorption bands, however, are symmetric with respect to a mirror line in the frequency-versus-extinction plot, for zero stress as well as for stresses for which no splitting occurs. We have assumed that the bands are also symmetric in cases where splitting does occur. The frequency of the band to be identified as the energy difference between levels has been taken to be the frequency of the mirror line.

The plots of the frequency shifts versus the magnitude of the applied pressure for different directions of stress and polarization all show a linear relationship within experimental error (see Fig. 2). The slopes therefore simply define the frequency-stress derivatives at zero pressure. The results are given in Table I together with the observed polarization character of the absorption bands.

III. INTERPRETATION

A. Group theory

When an impurity is substituted at a lattice site of a crystal lattice, the symmetry relevant for the vibrational transitions of the impurity is determined by both the symmetry of the impurity and the symmetry of the site. More precisely, one has to determine the irreducible representation of the point group L formed by the elements the site group S and the molecular point group of the impurity M have in common. The coincidence of elements depends largely on the orientation of the impurity at the lattice site. Therefore the resulting point group L, which has to be a subgroup of S and of M, also depends on this orientation. This dependence leads to a kind of degeneracy because one can put an ion of which the molecular point group is M onto an empty lattice site of site group S in a number of equivalent but different ways.

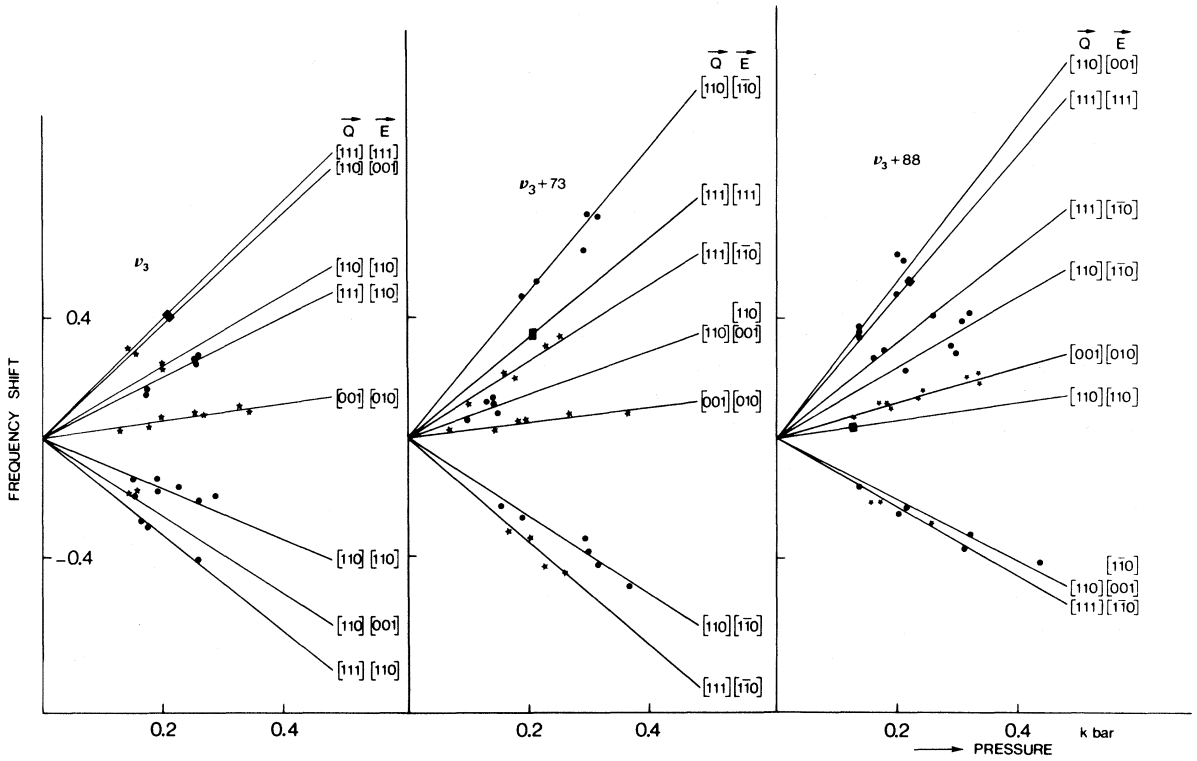

FIG. 2. Frequency shift vs pressure for various pressure and polarization directions for the internal vibration ν_3, the combination with the 73-cm^{-1} gap mode, and the combination with the 88-cm^{-1} gap mode.

This equivalence has been called orientational degeneracy.[8] The multiplicity of the orientational degeneracy is defined as the number of positions and orientations to which an impurity can be sent by the symmetry operations of the site group. This number can be found by dividing the order of the site group by the order of the resulting point group L.

The interpretation of the spectra of crystals with impurities under uniaxial stress can become very complicated because besides the lifting of the normal degeneracies of the vibrational levels as a consequence of lowered symmetry there is the possibility of lifting the orientational degeneracies. This may cause a multitude of different levels and hence the appearance of very complicated band structures. It is therefore necessary to keep full account of joined consequences of symmetry lowering.

We are here interested in the case of a substitutional impurity of D_{3h} symmetry in an O_h^5 lattice which deforms under uniaxial stress into a D_{4h}^{17}, a D_{3d}^4, or a D_{2h}^{25} lattice. All the possible sites of the O_h^5 space group give rise to only seven possible point groups L, i.e., D_3, C_{3v}, C_3, C_{2v}, C_2, C_5, and C_1. Studies of the infrared spectra of the KI: NO_3 system have been reported in the literature. Although different authors disagree[4,7,9] in their opinion about the choice between the possibilities D_3, C_{3v}, or C_3, it seems quite well established that the nitrate ion must be at a O_h site or slightly displaced along the [111] axis at a C_{3v} site and that the threefold axis of the NO_3^- ion coincides with the cube diagonal of the KI unit cell.

Table II shows the correlation between these point groups and the point groups which arise when the symmetry is lowered by an uniaxial stress parallel to the [111], the [001], or the [110] cubic crystal axes. It also shows to what extent the orientational degeneracy is lifted.

By standard group-theoretical methods one can now determine the different possible transitions

TABLE I. Frequency-stress derivatives in cm^{-1}/kbar and the qualitative polarization character of the internal vibration band and the combinations thereof with the gap modes, for different stress directions.

σ Zero pressure	ν_3 1372.50 cm^{-1}	ν_3+73 1445.42 cm^{-1}	ν_3+88 1460.44 cm^{-1}
[001]	0.29 [010]	0.27 [010]	0.58 [010]
[110]	2.0 [001]	2.5 [1$\bar{1}$0]	2.7 [001]
	−0.8 [1$\bar{1}$0]	0.7 [001]	1.2 [1$\bar{1}$0]
	−1.3 [001]	−1.3 [1$\bar{1}$0]	−1.0 [001]
			−1.0 [1$\bar{1}$0]
[111]	1.0 [1$\bar{1}$0]	1.3 [1$\bar{1}$0]	1.7 [1$\bar{1}$0]
	−1.6 [1$\bar{1}$0]	−1.7 [1$\bar{1}$0]	−1.2 [1$\bar{1}$0]

TABLE II. Unit-cell group of a O_h^5 crystal under uniaxial stress and some of the resulting point groups L for a D_{3h} impurity in such a crystal. The multiplicity of the orientational degeneracy is indicated.

$\vec{\sigma}\parallel[111]$	$4D_{3d}$	$C_{3v}(2)+C_s(6)$	$D_3(2)+C_2(6)$	$C_3(4)+C_1(12)$	$2C_s(6)+C_1(12)$	$4C_1(12)$
hydrost	O_h	$C_{3v}(8)$	$D_3(8)$	$C_3(16)$	$C_s(24)$	$C_1(48)$
$\vec{\sigma}\parallel[001]$	$3D_{4h}$	$C_s(8)$	$C_2(8)$	$C_1(16)$	$C_s(8)+C_1(16)$	$3C_1(16)$
$\vec{\sigma}\parallel[110]$	$6D_{2h}$	$2C_s(4)$	$2C_2(8)$	$2C_1(8)$	$4C_s(4)$	$6C_1(8)$

that may contribute to the spectrum. The fact that the magnitude of the frequency shifts of the different transitions is governed by a number of basic quantities which is limited by the symmetry of the problem, provides an additional very important expedient for a correct interpretation of the spectra. This more quantitative aspect requires some simple perturbation calculus.

B. Perturbation method

The perturbation V which appears in the Hamiltonian can be developed in terms of the strains[10]

$$V=\sum_{i,k} V_{ik}\,\epsilon_{ik}\,. \tag{1}$$

The matrix elements entering into the secular equations for the first-order perturbation have the form

$$\langle\phi_m|V|\phi_n\rangle=\sum_{i,k}\langle\phi_m|V_{ik}|\phi_n\rangle\epsilon_{ik}\,. \tag{2}$$

Because the shifts depend solely on these matrix elements, the number of independent matrix elements equals the number of parameters necessary for a full description of the shifts. This number can easily be found for different possible point groups. Under C_3, C_{3v}, D_3, and D_{3h} any *stress* induced shift of a nondegenerate level can be described with two independent parameters, whereas for degenerate levels this number is three under D_{3h}, four under D_3 and C_{3v}, and six under C_3.

For a nondegenerate level the first-order correction to the energy is given by

$$\Delta E=\sum_{ij}\langle A|V_{ij}|A\rangle\epsilon_{ij}\,. \tag{3}$$

One can write

$$\sum_{ij} V_{ij}\epsilon_{ij}=\sum_{\Gamma}\sum_{l} V(\Gamma)_l\,e(\Gamma)_l\,, \tag{4}$$

where $V(\Gamma)_l$ and $e(\Gamma)_l$ transforms according to the lth row of the Γ representation. Labeling the strain components e in the usual way one can specify

$$\sum_{ij} V_{ij}\epsilon_{ij}=V_1^*(A_1)(e_1+e_2+e_3)+V_2^*(A_1)(2e_3-e_2-e_1)+\sum_{\Gamma}{}'\sum_{l} V(\Gamma)_l\,e(\Gamma)_l\,. \tag{5}$$

The non-totally-symmetric representations of the relevant point groups give zero contributions and hence

$$\Delta E=\langle A|V_1^*(A_1)|A\rangle(e_1+e_2+e_3)+\langle A|V_2^*(A_1)|A\rangle(2e_3-e_2-e_1)\,. \tag{6}$$

Here e_1, e_2, and e_3 are defined with respect to the trigonal system. Transformation to the cubic system for the four situations that may arise when the threefold axis of the nitrate ion coincides with any of the cube diagonals gives rise to four equations. Denoting $\langle A|V_1^*(A_1)|A\rangle$ by T and $-\langle A|V_2^*(A_1)|A\rangle$ by C we obtain

$$\begin{aligned}
\Delta E(111)&=T(e_1+e_2+e_3)-C(e_4+e_5+e_6)\,,\\
\Delta E(11\bar{1})&=T(e_1+e_2+e_3)-C(e_4-e_5-e_6)\,,\\
\Delta E(1\bar{1}1)&=T(e_1+e_2+e_3)-C(-e_4-e_5+e_6)\,,\\
\Delta E(\bar{1}11)&=T(e_1+e_2+e_3)-C(-e_4+e_5-e_6)\,,
\end{aligned} \tag{7}$$

To express the shifts of the degenerate levels transforming according to an E representation one has to solve a secular equation of the form

$$0=\begin{vmatrix}\sum_{ij}\langle E_1|V_{ij}|E_1\rangle\epsilon_{ij}-\Delta E & \sum_{ij}\langle E_1|V_{ij}|E_2\rangle\epsilon_{ij}\\ \sum_{ij}\langle E_2|V_{ij}|E_1\rangle\epsilon_{ij} & \sum_{ij}\langle E_2|V_{ij}|E_2\rangle\epsilon_{ij}-\Delta E\end{vmatrix}. \tag{8}$$

This secular equation can be worked out in terms of the independent nonzero matrix elements, six in number when the resulting point group would be C_{3v} or D_3. Again a transformation from the trigonal to the cubic system should be applied, whereupon the first-order correction to the degenerate levels can be expressed in terms of the cubic strains and the totally symmetric matrix elements. An outline of this method has been given by Silsbee[11] for the limiting case of C_{3v} or D_3 symmetry. Although a quantitative comparison between the experimental data and the theoretical expressions with only four independent parameters are quite adequate, we shall start with the general expressions.

To proceed it is necessary to transform the expressions for the energy-level shifts into expressions containing the stresses instead of the strains. One can use the cubic compliances[5] and thus ob-

tain for the nondegenerate levels

$$\vec{\sigma}\parallel[001]:\quad \Delta E = T(S_{11}+2S_{12})\,\sigma\,; \tag{9a}$$

$$\vec{\sigma}\parallel[110]:\quad \Delta E[T(S_{11}+2S_{12})-\tfrac{1}{2}CS_{44}]\sigma\,, \tag{9b}$$

$$\Delta E = [T(S_{11}+2S_{12})+\tfrac{1}{2}CS_{44}]\sigma\,; \tag{9c}$$

$$\vec{\sigma}\parallel[111]:\quad \Delta E = [T(S_{11}+2S_{12})-CS_{44}]\sigma\,, \tag{9d}$$

$$\Delta E = [T(S_{11}+2S_{12})+\tfrac{1}{3}CS_{44}]\sigma\,; \tag{9e}$$

whereas for the degenerate levels the general expressions are

$\vec{\sigma}\parallel[001]$:

$$\Delta E = [T(S_{11}+2S_{12})+\tfrac{1}{3}(p^2+r^2)^{1/2}(S_{11}-S_{12})]\sigma\,, \tag{10a}$$

$$\Delta E = [T(S_{11}+2S_{12})-\tfrac{1}{3}(p^2+r^2)^{1/2}(S_{11}-S_{12})]\sigma\,; \tag{10b}$$

$\vec{\sigma}\parallel[110]$:

$$\Delta E = (T(S_{11}+2S_{12})+\tfrac{1}{3}\{[p(S_{11}-S_{12})-qS_{44}]^2 + [r(S_{11}-2S_{12})-sS_{44}]^2\}^{1/2}-\tfrac{1}{2}CS_{44})\,\sigma\,, \tag{10c}$$

$$\Delta E = (T(S_{11}+2S_{12})-\tfrac{1}{3}\{[p(S_{11}-S_{12})-qS_{44}]^2 + [r(S_{11}-2S_{12})-sS_{44}]^2\}^{1/2}-\tfrac{1}{2}CS_{44})\,\sigma\,, \tag{10d}$$

$$\Delta E = (T(S_{11}+2S_{12})+\tfrac{1}{3}\{[p(S_{11}-S_{12})+qS_{44}]^2 + [r(S_{11}-2S_{12})+sS_{44}]^2\}^{1/2}+\tfrac{1}{2}CS_{44})\,\sigma\,, \tag{10e}$$

$$\Delta E = (T(S_{11}+2S_{12})-\tfrac{1}{3}\{[p(S_{11}-S_{12})+qS_{44}]^2 + r(S_{11}-2S_{12})+sS_{44}]^2\}^{1/2}+\tfrac{1}{2}CS_{44})\,\sigma\,; \tag{10f}$$

$\vec{\sigma}\parallel[111]$:

$$\Delta E = [T(S_{11}+2S_{12})-CS_{44}]\sigma\,, \tag{10g}$$

$$\Delta E = [T(S_{11}+2S_{12})+\tfrac{4}{9}S_{44}(q^2+s^2)^{1/2}+\tfrac{1}{3}CS_{44}]\sigma\,, \tag{10h}$$

$$\Delta E = [T(S_{11}+2S_{12})-\tfrac{4}{9}S_{44}(q^2+s^2)^{1/2}+\tfrac{1}{3}CS_{44}]\sigma\,; \tag{10i}$$

where $p=B+A\sqrt{2}$, $q=B-\frac{1}{2}A\sqrt{2}$, $r=G+H\sqrt{2}$, and $s=G-\frac{1}{2}H\sqrt{2}$ in terms of the totally symmetric matrix elements A, B, G, and H. A considerable simplification is obtained under D_3 or C_{3v} when $H=G=0$, and under D_{3h} even $H=G=A=0$.

It is clear that for a transition from the totally symmetric ground state to a nondegenerate excited state, the frequency shift $\Delta(\hbar\omega)$ will be given by an expression of exactly the same form as that for the level shift. Furthermore, the expressions for the energy shift of the nondegenerate level appear also as terms in the expressions for the energy shift of the degenerate level. Hence the expressions for the degenerate-level shift are also valid for the frequency shift of a transition to a degenerate excited level. The experimentally determined frequency-stress derivatives are therefore given by expressions (9) and (10). The coupling coefficients are now the differences between the corresponding coupling coefficients in the expressions for the level shifts. Physically these coupling coefficients can be interpreted as the cubic terms in the series development of the potential energy such as

$$T(A_1)=\frac{1}{2\omega}\,\frac{\delta^3\phi}{\delta u^2\,\delta(e_1+e_2+e_3)}\,.$$

C. Results

To come to an interpretation of the experimental data one should first consider the effect of the applied stresses on the internal transition of the nitrate ion. In principle one can insert the experimentally determined frequency-stress derivatives into Eq. (10) to find the values of the matrix elements A, B, T, C, G, and H. However, the identification of the multitude of bands that appear in the spectra when pressure in different directions is applied poses quite a problem. Considering the total number of bands one surmises that the use of six parameters instead of four would not give any significantly better results. We therefore consider the system to be of C_{3v} or D_3 symmetry and omit the matrix elements G and H. Four independent parameters give rise to nine equations for stresses in the [001], [110], and [111] directions. Every equation corresponds to a band shift. On the basis of these equations one therefore expects two different band shifts for [001] *stress*, four for [110] *stress*, and three for [111] *stress*. Experimentally we only found one, three, and two shifting bands for the different pressure directions, respectively. To come to an assignment we applied a least-squares fit to all the $2!\,4!\,3! = 288$ possible permutations. For only 12 possibilities did the mean residue fall within the experimental error. Comparing the qualitative polarization characteristics of the experimentally determined bands, with the prediction of the polarization ratios,[11] only one possibility survived. The ensuing equations and the solutions for the four matrix elements are given in Table III. It is to be noted that according to the favored solution, the internal vibration of the nitrate ion which combines with the gap modes shows a splitting under stress because of lifting of the rotational degeneracy as well as because of lifting of the normal degeneracy. So does [111] stress give rise to a splitting into [111] oriented NO_3^- ions on one hand and a group of $[1\bar{1}1]$, $[11\bar{1}]$, and $[\bar{1}11]$ oriented ions on the other hand. For this last group the degeneracy of the E-type level is lifted and the net result is three bands at different frequencies.

We can now proceed by taking the best fit of the shifted frequencies of the internal vibration as the

TABLE III. Experimentally determined band shifts in cm^{-1}/kbar, the calculated best fit, the theoretical polarizations, and the experimental polarization character for nitrate ions in different orientations according to Eqs. (10a)–(10i).

Eq.	Expt.	Calc.	E relative intensities			E expt.	Impurity orientation
			[100]	[010]	[001]		
(10a)	•••	0.38	$\frac{2}{3}$	$\frac{2}{3}$	$\frac{8}{3}$	•••	{[111] [11$\bar{1}$]}
(10b)	0.29	0.32	2	2	0	[010]	{[1$\bar{1}$1] [$\bar{1}$11]}
			[110]	[1$\bar{1}$0]	[001]		
(10c)	−0.80	−0.73	0	2	0	[1$\bar{1}$0]	{[111] [11$\bar{1}$]}
(10d)	2.0	2.00	$\frac{2}{3}$	0	$\frac{4}{3}$	[001]	
(10e)	•••	1.46	2	0	0	•••	{[1$\bar{1}$1] [$\bar{1}$11]}
(10f)	−1.3	−1.33	0	$\frac{2}{3}$	$\frac{4}{3}$	[001]	
			[111]	[1$\bar{1}$0]	[11$\bar{2}$]		
(10g)	1.0	0.92	0	1	1	[1$\bar{1}$0]	{[111]}
(10h)	•••	2.00	$\frac{8}{3}$	$\frac{1}{6}$	$\frac{1}{6}$	•••	{[11$\bar{1}$] [1$\bar{1}$1] [$\bar{1}$11]}
(10i)	−1.6	−1.68	0	$\frac{3}{2}$	$\frac{3}{2}$	[1$\bar{1}$0]	

$T(S_{11}+2S_{12}) = 0.347$ $(A\sqrt{2}+B)(S_{11}-S_{12}) = 0.43$

average deviation 0.085

$(\frac{1}{2}A\sqrt{2}-B)S_{44} = -4.14$ $CS_{44} = -0.57$

zero point for the shifts of the frequencies of the combination bands. Since the number of observed combination-band shifts does not exceed the number of internal-band shifts, the matrix elements G', H', A', and B' for the gap mode shifts have to be assumed to be zero. Furthermore, the values of the combination-band shifts tend to be grouped within 0.5 cm^{-1}/kbar around the values of the internal-band shifts as can be seen in Table I. Of course one does not know beforehand which of the combination-band shifts corresponds to which of the zero points within the series obtained with one stress direction, and this group formation might be coincidence. If not, the shifts of the gap modes proper are very small indeed. The errors of the determination of the internal-band shift and the combination-band shift add and must be estimated to be ± 0.4 cm^{-1}/kbar. It would therefore be impossible to find a meaningful solution to Eq. (9) and (10). We shall therefore proceed by looking for predictions of the values of the matrix elements from theoretical calculations. One may then compare the predicted band shifts with the experimental data in a more direct way.

IV. CALCULATIONS

In the preceding sections it was shown how the experimentally determined frequency-stress derivatives can be related with the frequency-strain derivatives by the use of the compliances appropriate for the host crystal. If one wants to find the connection with microscopic model calculations one has to make the assumption that the local compliances around the impurity are given by the bulk compliances. In that case one can relate the strain components, as appearing in the frequency-strain derivatives, with the static relaxation of the ions around the impurity. The matrix element T is given by $d\omega/d(e_1+e_2+e_3) = \frac{1}{3}d\omega/dr$, where r is the distance between the impurity and the six neighboring particles. C is given by $d\omega/d(e_4+e_5+e_6) = \frac{1}{3}d\omega/d\theta$, where θ is the angle between the x', y', and z' axes of the deformed unit cell around the impurity.

We now use a Green's-function method to calculate the gap-mode frequencies. This method has been outlined by several authors and has been in wide use for systems with monatomic impurities[12–14]. The new degrees of freedom which are introduced by a polyatomic impurity do not effect the applicability of the method.[15] The variables can be separated into a set comprising the molecular mass and the coordinate of the center of mass, and a set comprising the reduced masses and coordinates of the molecular system.

Neglect of the coupling between the translational and rotational motion leads to exactly the same equation of motion for the polyatomic impurity as for a monatomic impurity, $(L+\delta L)u = 0$. The gap-mode frequencies are found as a solution of the equation

$$\mathrm{Re}[\mathrm{Det}(I+G\cdot L)] = 0,$$

where I is the unit matrix, G is the Green's function for the unperturbed crystal, and δL gives the

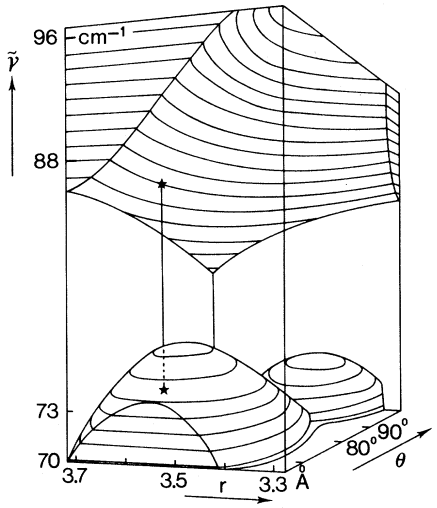

FIG. 3. Calculated gap-mode frequencies for a KI lattice with an impurity of mass 62, given as a function of the angular and the radial relaxation of the lattice around the impurity.

change in the dynamical matrix upon introduction of the impurity. $\delta L = [\omega^2(M' - M_0) + \Delta\phi]$ and contains a 21×21 force-constant matrix when only the interaction with the six neighboring ions is taken into account. This can be reduced because the matrix must be invariant under the point group which is generated when the impurity is put at the lattice site.

Usually one assumes that the potential has the Born-Mayer shape $\phi = \lambda e^{-r/\rho}$; the central and noncentral force constants then take the form

$$A = (-\lambda/\rho^2)\, e^{-r/\rho} \quad \text{and} \quad B = (\lambda/r\rho)\, e^{-r/\rho}.$$

We insert quite arbitrarely the values for λ and ρ that are appropriate for KI.[16] Deviations from these force constants will then be found in a formal deviation of r, the radial relaxation, and a changed ratio between A and B, the angular relaxation. Interpretation in terms of changed λ and ρ or true relaxation can be made after the actual calculations. Use was made of the eigendata of KI, 1000 points in the first Brillouin zone, that have been obtained by a shell-model calculation.[17] These

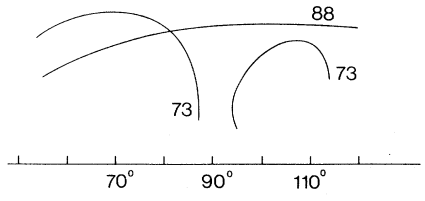

FIG. 4. Values of the angular vs the radial relaxation for the calculated gap-mode frequencies at 73 and at 88 cm^{-1}.

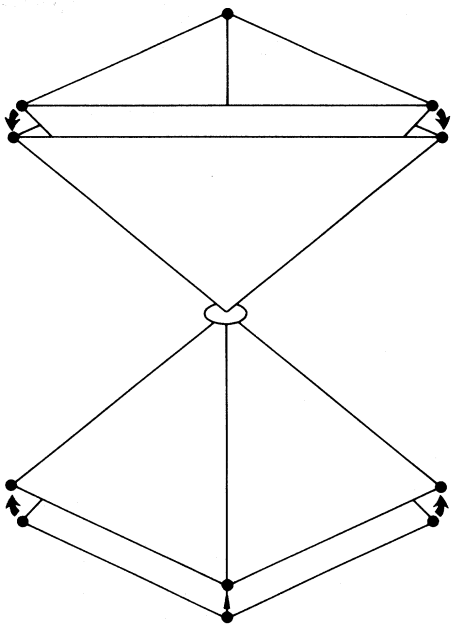

FIG. 5. Relaxation of the six potassium ions around the nitrate ion.

were kindly made available to us by Cowley.

A region of positive and negative relaxation around the values of r and θ in the unperturbed KI lattice, i.e., $r = 3.526$ Å and $\theta = 90°$, was scanned for solutions that gave a gap mode. A general impression of the results can be obtained from Fig. 3. First it should be noted that without relaxation of the lattice, in the isotopic substitution model, only one gap mode, a raised acoustic mode at 72 cm^{-1}, is predicted. This result has been obtained before.[4] Agreement with the two gap modes which are found experimentally is obtained when allowance is made for relaxation of the lattice. Only then do solutions for a second gap mode emanate from the optical branches. It is easy to find a value for the angular deformation and for the radical relaxation for which two gap modes at 73 and 88 cm^{-1} occur. From Fig. 4 it can be seen that $\theta = 81° 40'$ and $r = 3.67$ Å give the only solution with realistic values for the relaxation, Fig. 5. For this solution one can subsequently determine the derivatives of the gap-mode frequencies with respect to the angular and the radical relaxation. The values are $T(73) = -81$, $T(88) = -100$, $C(73) = -11$, and $C(88) = 1.5$ cm^{-1}. With the insertion of the bulk compliances[18] of KI, $S_{11} = 38.3 \times 10^{-13}$, $S_{44} = 270 \times 10^{-13}$, and $S_{12} = -5.4 \times 10^{-13}$ $cm^2\,dyn^{-1}$, one can calculate the frequency-stress derivatives according to Eqs. (9) and (10). A comparison with the experimental data can now be made by adding the calculated shifts of the gap-mode frequencies to the experimentally determined shifts of the internal vibration as determined by

TABLE IV. Calculated combination band shifts of the 73 and the 88-cm^{-1} gap modes compared with a tentative assignment of the experimental band shifts.

Eq.	Total shift 73 Calc.	Total shift 73 Expt.	Total shift 88 Calc.	Total shift 88 Expt.
(10a)	0.16	0	0.10	
(10b)	0.10	0.3±0.4	0.04	0.6±0.4
(10c)	−0.80		−1.03	−1.0±0.4
(10d)	1.93	2.5±0.4	1.70	2.7±0.4
(10e)	1.07	0.7±0.4	1.20	1.2±0.4
(10f)	−1.70	−1.3±0.4	−1.59	−1.0±0.4
(10g)	1.00		0.60	
(10h)	1.68	1.3±0.4	1.73	1.7±0.4
(10i	−2.00	−1.7±0.4	−1.95	−1.2±0.4

the least-squares fit, Table III. The resulting combination-band shifts are given in Table IV, where a comparison is made with a tentative assignment of the experimental data. It should be noted that measurements with polarized radiation are of little help for the assignment of the combination bands which practically all have a mixed polarization character. One exception is the 73-cm^{-1} gap mode under [111] pressure. This example is shown in Figs. 6 and 7.

V. DISCUSSION

The use of the isotopic substitution model with radial and angular relaxation does give an excellent prediction on the gap-mode behavior in the system KI : NO_3^-. First of all the model predicts that one gap mode should be a slightly raised acoustic mode, whereas the other stems from the optical branches. The different origin of the two

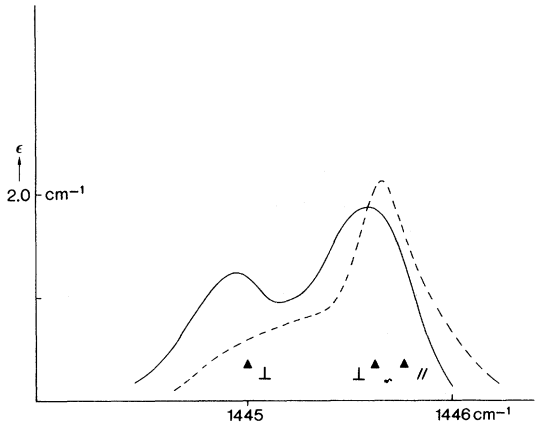

FIG. 6. 73-cm^{-1} gap-mode combination band with stress applied in the [111] direction measured with the polarization vector perpendicular (solid line) and parallel (dashed line) to the [111] direction. The triangles give the theoretical values of the band centers. Polarization character is indicated.

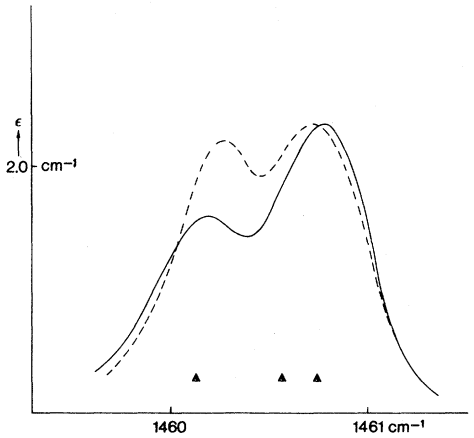

FIG. 7. 88-cm^{-1} gap-mode combination band with stress applied in the [111] direction measured with the polarization vector perpendicular (solid line) and parallel (dashed line) to the [111] direction. The triangles give the theoretical values of the band centers. Polarization is mixed for all bands.

gap modes is confirmed by the different optical behavior of the two modes in the far infrared.[6] In this spectral region a very intense absorption band has been observed at 88 cm^{-1} and a very weak absorption at 73 cm^{-1}.

Furthermore, the model predicts frequency-strain derivatives which, when modified into frequency-stress derivatives, give a reproduction of the stress dependence of the absorption spectra within the experimental error. Incidentally one notes that the shifts that are caused by the applied stresses are quite small, too small to present an altogether satisfactory means of determining the strains. As a matter of fact the model predicts the poor response. The mode Grüneisen constant which can be calculated from $\gamma = (1/\omega)d\omega/d(e_1+e_2+e_3)$ is only 1.11 for the 73-cm^{-1} and 1.14 for the 88-cm^{-1} mode. This is lower than the mode Grüneisen constant for the TO phonon of KI, which should be about 3, and the thermodynamic Grüneisen constant which is 1.5.[19] It is interesting to compare the change of the angle from 90° in KI to 81° 40′ around the NO_3^- ion, with the angle in rhombic KNO_3 III which is still smaller, 76° 56′. The edge is 3.526 in KI, 3.673 around the impurity, and 4.365 Å in rhombic KNO_3 (at 393 K). The deformed unit cell around the impurity is therefore an intermediate between the cubic KI and the comparable KNO_3 structure.[20]

All these agreements form a strong justification for the use of a model that takes lattice relaxation into account. One should realize that the way in which the relaxation of r and θ are operative in the model allows for an alternative interpretation in terms of an angle-dependent radius of the im-

purity ion. Since the parameter λ in the Born-Mayer potential contains $e^{[r(K^+)+r(NO_3^-)]/\rho}$ our results tell us that the radius of the nitrate ion, as measured along the line connecting the centers of mass of the nitrate ion and a potassium ion, is $r(I^-) - \Delta r = 2.04$ Å. The redistribution of central and noncentral forces cannot only be interpreted in terms of an angle change between the axes, but also as if it meant that the surface of the nitrate ion at the point of intersection with the connection line deviates $90° - 81° 40' = 8° 20'$ from a spherical surface. The result, a disk-shaped nitrate ion, is not very surprising, of course. The method which we used here constitutes, however, a new and promising way of probing the angle dependent potential between ions in a crystal.

ACKNOWLEDGMENT

The work described here is part of the research program of the Foundation for Fundamental Research of Matter (F.O.M.) and was made possible by financial support from the Netherlands Organization for Pure Research (Z.W.O.).

[1]G. Schaefer, J. Phys. Chem. Solids 12, 233 (1960).
[2]A. A. Maradudin, Solid State Phys. 18, 273 (1965); 19, 1 (1966).
[3]A. J. Sievers, *Localized Excitations in Solids* (Plenum, New York, 1968), p. 34.
[4]R. Metselaar and J. van der Elsken, Phys. Rev. 165, 359 (1968).
[5]I. G. Nolt and A. J. Sievers, Phys. Rev. 174, 1004 (1968).
[6]K. F. Renk, Phys. Lett. 14, 281 (1965).
[7]R. K. Eynthoven and J. van der Elsken, Phys. Rev. Lett. 23, 1455 (1969).
[8]A. A. Kaplyanskii, Opt. Spectrosc. 16, 557 (1964).
[9]L. K. Frevel, Spectrochim. Acta 15, 557 (1959).
[10]A. A. Kaplyanskii, Opt. Spectrosc. 16, 329 (1964).
[11]R. H. Silsbee, Phys. Rev. 138, A180 (1965).
[12]G. Benedek and A. A. Maradudin, J. Phys. Chem. Solids 29, 423 (1968).
[13]D. Bäurle and R. Hübner, Phys. Rev. B 2, 4252 (1970).
[14]C. de Jong, G. H. Wegdam, and J. van der Elsken, Phys. Rev. B 8, 4868 (1973).
[15]M. Wagner, Phys. Rev. 131, 2520 (1963); 133, A750 (1964).
[16]M. Born and K. Huang, *Dynamical Theory of Crystal Lattices* (Oxford U.P., London, 1954).
[17]G. Dolling, R. A. Cowley, G. Schittenhelm, and I. M. Thorson, Phys. Rev. 147, 577 (1966).
[18]Landolt Börnstein, *Numerical Data and Functional Relationships III*2 (Springer, Berlin, 1969).
[19]R. Ruppin and R. W. Roberts, Phys. Rev. B 3, 1406 (1971).
[20]T. F. M. Barth, Z. Phys. Chem. B 43, 448 (1938).